SERI/STR-211-2607
(DE85008810)

PHOTOVOLTAIC DEVICES USING HYDROGENATED AMORPHOUS SILICON PRODUCED BY THE CHEMICAL VAPOR DEPOSITION OF HIGHER ORDER SILANES

Final Report, August 1, 1983—August 31, 1983

By
A. Delahoy

April 1985

Work Performed Under Contract No. AC02-83CH10093

Chronar Corporation
Princeton, New Jersey

and

Solar Energy Research Institute
Golden, Colorado

Technical Information Center
Office of Scientific and Technical Information
United States Department of Energy

DISCLAIMER

Available from the National Technical Information Service, U. S. Department of Commerce, Springfield, Virginia 22161.

Price: Printed Copy A03
Microfiche A01

Codes are used for pricing all publications. The code is determined by the number of pages in the publication. Information pertaining to the pricing codes can be found in the current issues of the following publications, which are generally available in most libraries: *Energy Research Abstracts (ERA); Government Reports Announcements* and Index *(GRA* and I); *Scientific and Technical Abstract Reports (STAR);* and publication NTIS-PR-360 available from NTIS at the above address.

Printed in the United States of America
USDOE Office of Scientific and Technical Information
Oak Ridge, Tennessee

SERI/STR-211-2607
(DE85008810)
Distribution Category UC-63

Photovoltaic Devices Using Hydrogenated Amorphous Silicon Produced by the Chemical Vapor Deposition of Higher Order Silanes

Final Report
1 August 1982 - 31 August 1983

A Subcontract Report

A. Delahoy
Chronar Corporation
Princeton, New Jersey

April 1985

Prepared under Subcontract No. XL-2-02181-1

SERI Technical Monitor: B. Stafford

Solar Energy Research Institute
A Division of Midwest Research Institute

1617 Cole Boulevard
Golden, Colorado 80401

Prepared for the
U.S. Department of Energy
Contract No. DE-AC02-83CH10093

EXECUTIVE SUMMARY

Hydrogenated amorphous silicon (a-Si:H) films were prepared by the static chemical vapor deposition (CVD) of mainly disilane. The disilane was prepared in-house by a chemical method and by the silent electric discharge of monosilane for high purity disilane. Deposition temperatures were generally in excess of 400 °C. At 450 °C growth rates as high as 10 angstroms per second were observed. Based upon NO scavenging reactions, silyl radicals are not expected to be an important source of film growth. At the high CVD temperatures, it was orginally expected that the relatively high gap state density of this material stemmed from a low atomic percent hydrogen within the films. However, by the nuclear reaction technique, the hydrogen content is about 14 %. The hydrogen concentration within a film was found to oscillate as a consequence of the successive static depositions and the changing extent of reaction within each deposition. This changing hydrogen content is expected to interfere with carrier transport.

Residual dopants, contaminants within the disilane, and system contaminants, as expected, affect the properties of a-Si:H material. Surprisingly, in the case of ppm phosphorous doping, early work suggested that the mobility-lifetime product for electrons could be improved without substantially affecting the mobility-lifetime product for holes. Later experiments indicated a loss in the mobility-lifetime product for holes.

The photoconductivity of the CVD material increased with decreasing activation energy ($E_C - E_F$). At an activation energy of 0.58 the mobility-lifetime product for electrons determined from the photoconductivity was 2.2×10^{-7} cm^2V^{-1}. The temperature dependence of the photoconductivity only exhibits a single high temperature peak. The spectral response of the photoconductivity shifts to longer wavelengths as the temperature increases.

An exponential sub-band gap absorption edge is observed. The inverse slope of this edge which is a measure of film disorder is roughly 68 meV or about 30 percent larger than in glow-discharge films. The ratio of the change in band gap to the change in inverse slope of the absorption edge was found to be the same regardless of whether the deposition temperature or measurement temperature was varied, strongly suggesting that the energy band gap is determined by the disorder.

At this time it is not known whether the greater disorder or gap state density of defects can be directly attributable to the high deposition temperature or whether it arises from contamination including contamination from the substrate because of the high deposition temperature.

The CVD material is easily doped either n or p type with dark conductivities around 10^{-3} $(ohm\text{-}cm)^{-1}$ and thermal activation energies of the dark conductivity around 0.2 eV. In addition, wide band gap p layers were deposited from methylsilanes.

All CVD pin devices were generally less than 1.5 % efficient, e. g., open-circuit voltage 0.62 V, short-circuit current density 5.9 ma/cm^2, and fill factor 0.4. In stacked CVD pin devices, efficiencies greater than 3 % have been observed.

A-Si:H films have been produced by the mercury sensitized photo CVD of disilane. This is expected to be a very promising new technique since low deposition temperatures are possible and since atomic hydrogen is produced.

TABLE OF CONTENTS

LIST OF ILLUSTRATIONS

LIST OF TABLES

ABSTRACT

This report presents the results of work performed to explore the properties of hydrogenated amorphous silicon (a-Si:H) produced by the chemical vapor deposition (CVD) of higher order silanes. The higher silanes were produced by a chemical method and by silent electric discharge of CCD-grade monosilane. The latter method yields a high-purity mixture of higher silanes. The a-Si:H films were deposited mainly from silane by a static CVD method: the heated reactor was purged and evacuated and then filled to the initial pressure desired with reactant gases. The extent of the deposition chemistry was monitored by the increase in pressure. At a predetermined increase in pressure, the system was quickly evacuated. This process was repeated several times to obtain a film of the desired thickness. These experiments were performed to increase our understanding of the deposition mechanism of a-Si:H, to improve the quality of CVD a-Si:H layers for device applications, to measure the properties of CVD a-Si:H doped and undoped layers, and to explore new device structures and alternative CVD techniques.

SECTION 1
INTRODUCTION

The work performed under this contract explored the properties of hydrogenated amorphous silicon (a-Si:H) produced by the chemical vapor deposition (CVD) of higher silanes. The higher silanes are produced at Chronar by a chemical method and also by silent electric discharge (SED) of CCD grade monosilane. The latter method yields a much higher purity mixture of higher silanes.

The a-Si:H films were mainly deposited from disilane by a static CVD method. In this method the heated reactor is purged and evacuated, and then filled to the desired initial pressure with the reactant gases. The extent of the deposition chemistry is monitored by the increase in pressure. At a predetermined increase in pressure the system is quickly evacuated. This process is generally repeated several times to obtain a film of desired thickness.

Experiments performed under this contract included the following objectives: (1) to increase our understanding of the deposition mechanism of a-Si:H, (2) to improve the quality of CVD a-Si:H i-layers for device application, (3) to measure the properties of CVD a-Si:H doped and undoped layers, and (4) to explore new device structures and alternative CVD techniques. The details and the results of these experiments are given in the following sections.

SECTION 2
HIGHER SILANES

2.1 SOURCE OF HIGHER SILANES

For most of the work performed under this contract, the higher silanes are produced from the addition of magnesium silicide to dilute acids, including hydrochloric acid. The silanes are then purified by trap to trap distillation. In an effort to improve the purity of the silanes, the higher silanes have also been produced by subjecting CCD grade silane to a silent electric discharge.

2.2 HIGH PURITY DISILANE

Research employing high purity disilane (produced by silent electric discharge) has been initiated to resolve the role of impurities in determining the electronic properties of CVD a-Si:H. Fig. 1 shows the dark conductivity versus 1/T for such a film. The activation energy ,DELTA E, is 0.67 eV (see Fig. 2). These preliminary measurements of majority carrier transport have not revealed any significant differences between these films and films prepared from disilane produced by the usual chemical methods. As the next step the photoconductivity of these films will be investigated. This will be followed by device optimization using the high purity disilane.

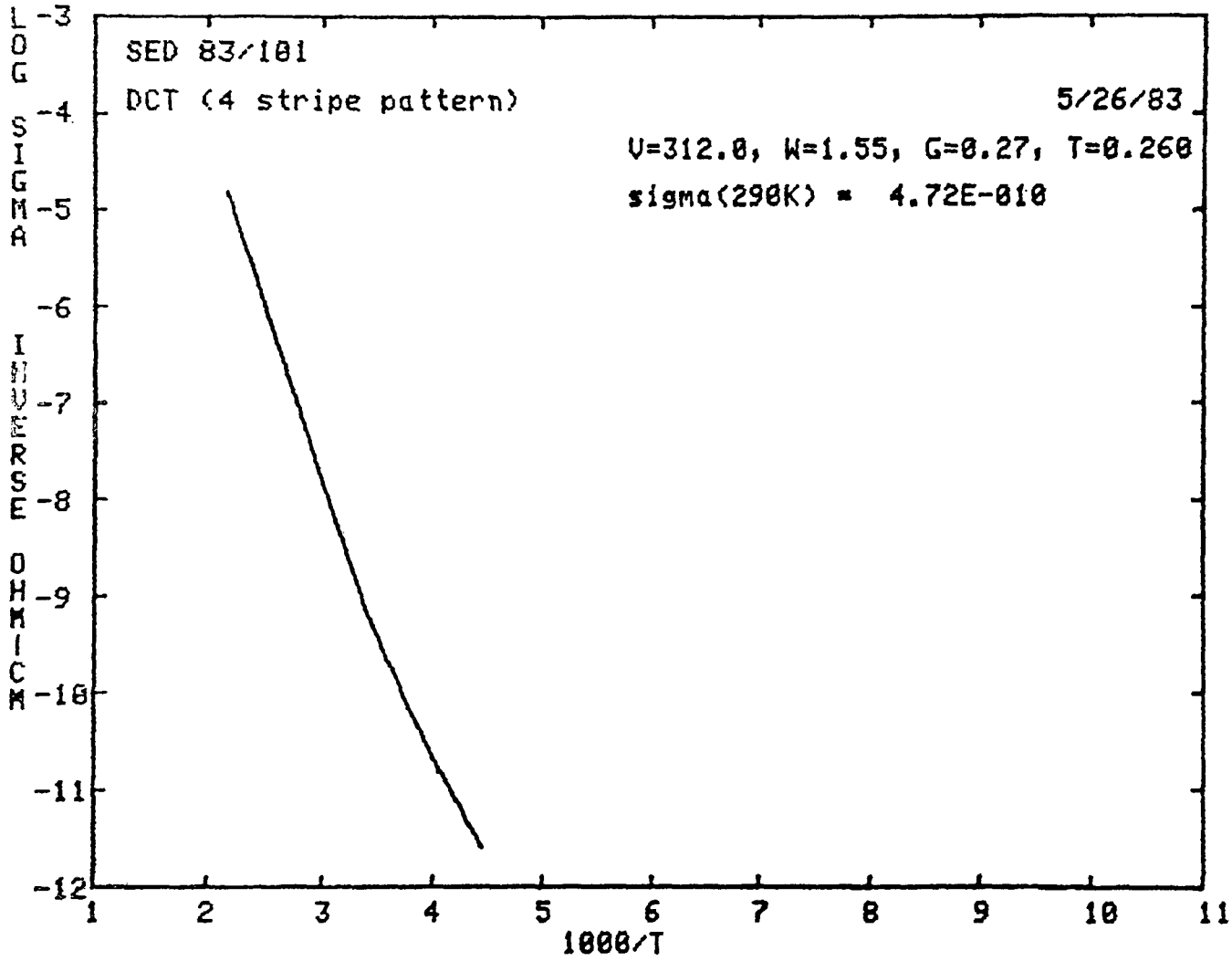

FIG. 1. Arrhenius plot of dark conductivity for an a-Si:H film deposited by CVD of high purity disilane.

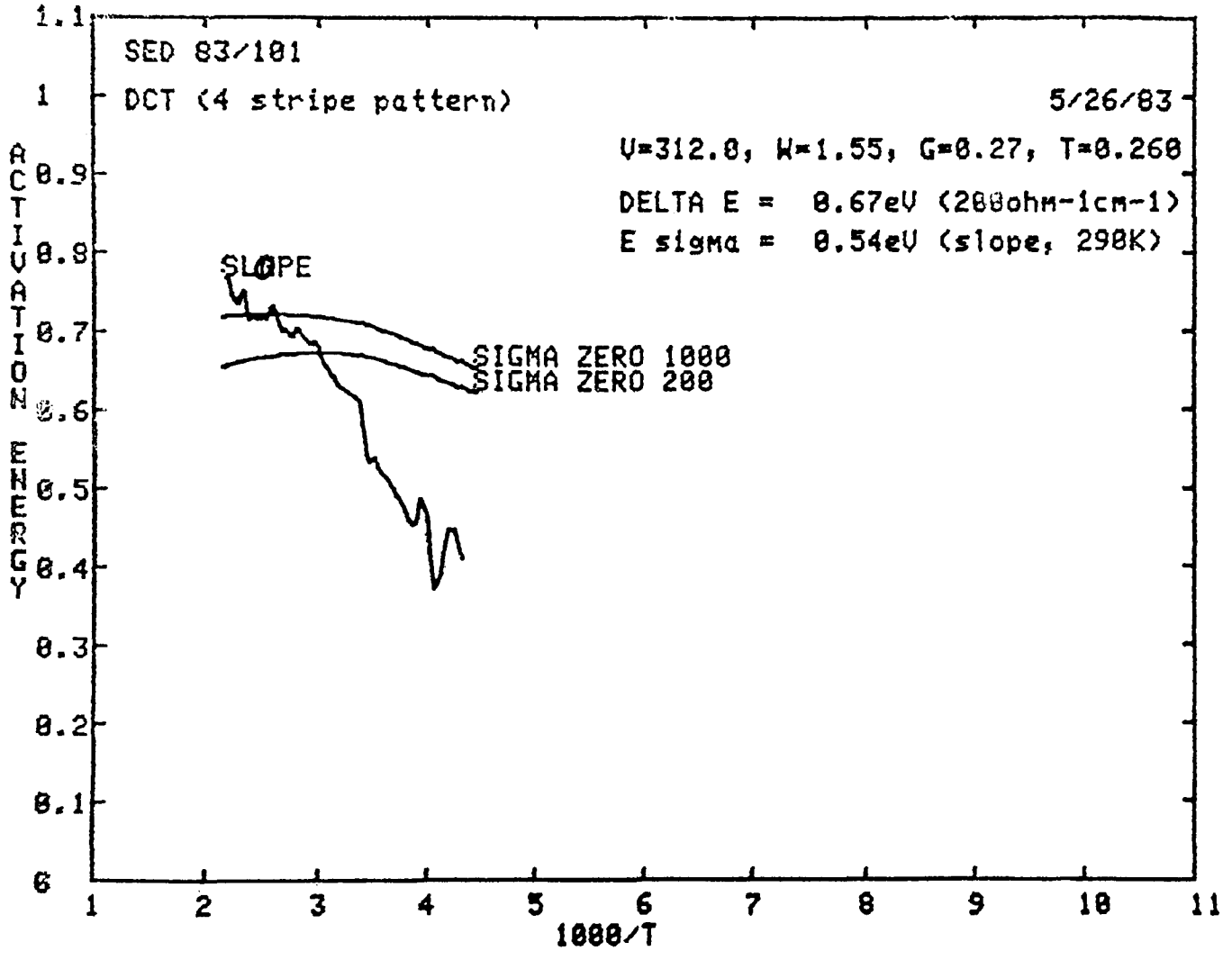

FIG. 2. Activation energies ΔE and E_σ versus inverse temperature of the film of Fig. 1.

SECTION 3
GROWTH MECHANISMS

3.1 DEPOSITION METHODS

Three basic deposition schemes, discussed below, illustrate that different growth mechanisms are possible for CVD films. It is expected that different properties are obtainable for the different deposition schemes.

1. HOMO-CVD films. These films are characterized by a substrate temperature significantly cooler than the surrounding gas temperature. B. Scott at IBM has investigated the properties of a-Si:H produced by this method.[1]

2. HETERO-CVD films. These films are characterized by comparable gas-phase and substrate temperature. It is expected that both gas-phase and surface reactions are important in this case. The films produced under this contract are mainly of this type.

3. SURFACE-CVD films. These films are characterized by a substrate temperature substantially greater than the gas-phase temperature. In practice, this condition can be obtained by very short gas-phase residence times, that is, a proper geometry and a high gas flow rate.

3.2 GROWTH RATES

Growth rates as high as 10 angstroms per second and producing specular films have been obtained. Different growth rates and associated activation energies were obtained depending on the starting gas and temperature profile. In one study for disilane and trisilane the substrate is hot, but not the surrounding walls. In this case the gas-phase temperature is not well defined, since the large temperature gradient (the gas-phase temperature rapidly decreases away from the substrate) may induce convection currents. The results of this study show (see Fig. 3) that a higher deposition rate is obtained for trisilane. At least at higher temperatures both disilane and trisilane had an activation energy of about 1.5 eV. Since the low temperature break in the slope for disilane is based on one point and not observed for trisilane (similar trends between di- and trisilane are expected), further experiments are necessary before one is justified in claiming a change in the activation energry for disilane around 410°C.

In another study using equal starting pressures and static deposition, an Arrhenius plot of the maximum deposition rate versus inverse temperature revealed different low (below 370°C) and high temperature activation energies (see Fig. 4). The respective activation energies are 2.56 and 1.95 eV.

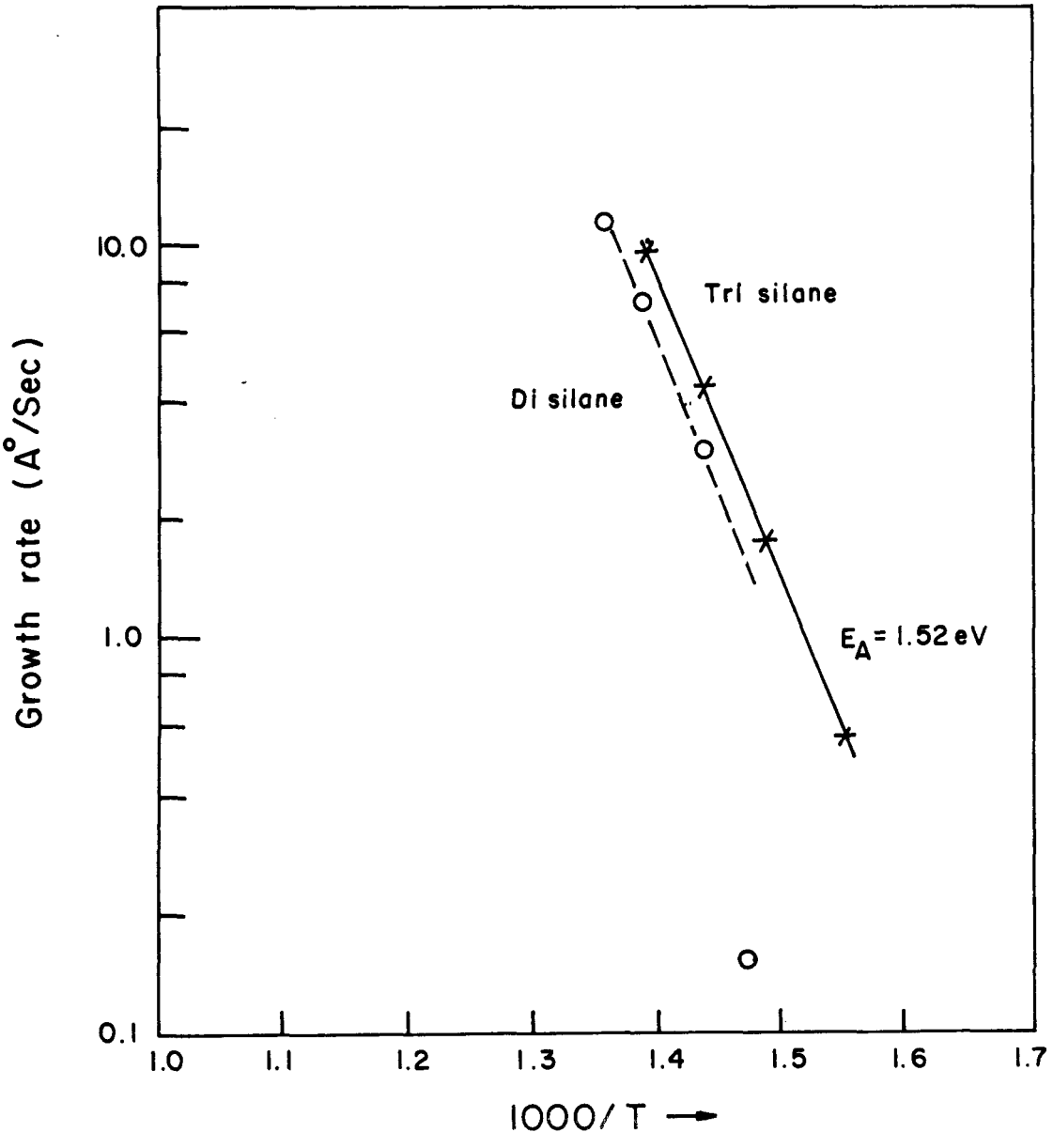

FIG. 3. Film growth rate from disilane and trisilane versus inverse temperature.

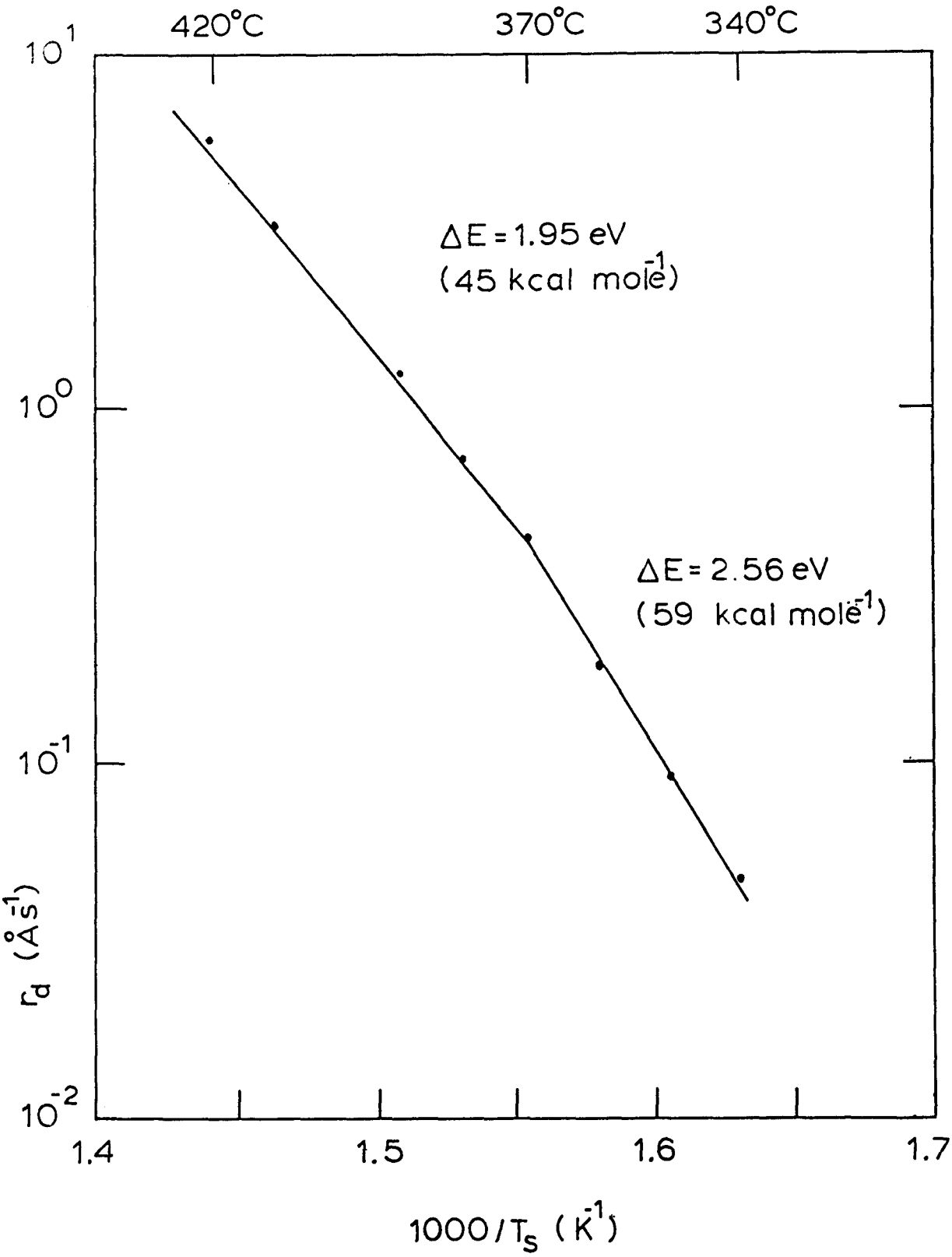

FIG. 4. Arrhenius plot of maximum deposition rate versus inverse temperature for the CVD of disilane in a static system.

3.3 TEST FOR SILYL RADICALS

In connection with our studies of the deposition mechanism of CVD a-Si:H we have investigated the effects of adding nitric oxide (NO) to the disilane. Nitric oxide is known to be an efficient scavenger of radicals having an unpaired spin. Thus it should be an efficient scavenger of silyl type radicals, e.g., SiH_3. Furthermore, if silyl type radicals participate in free-radical chain mechanisms, then the addition of a small amount of NO should dramatically decrease the reaction rate and corresponding deposition rate. The absence of any dramatic effect on the deposition rate (or the material properties) upon the addition of NO would support the contention that silyl radicals do not play a significant role in the gas-phase chemistry. Four a-Si:H films of nominally identical thickness (0.4 microns) were made with varying quantities of NO added. Table I summarizes the deposition parameters and the AM1 photoconductivity. Since one percent NO in helium was used, part of the observed decrease in the deposition rate is due to helium dilution. At the highest NO concentration used (0.5% NO), the helium dilution of the disilane could easily be the dominant reason for the decrease in growth rate. For free-radical chain mechanisms, there should be a large decrease in the growth rate in going from no addition of NO to a small addition of NO. On the other hand, there should only be a slight decrease between a large addition and a larger addition. Therefore, regarding the growth of the a-Si:H film, we conclude that a free-radical chain involving silyl type radicals is very unlikely. We further conclude from runs K4030 to K4032 that NO does not drastically cut the deposition rate, implying that silyl type radicals are not a major contributor to the film growth. There is a slight tendency for photoconductivity to decrease with increasing NO concentration. This is perhaps due to the reaction of NO with dangling bonds on the surface of the growing film, leading to the incorporation of oxygen and nitrogen in the film.

Table I. Deposition parameters and AM1 photoconductivity for films grown with different concentrations of NO added to the disilane.

run #	NO* (%)	T_s (^oC)	P (Torr)	dep. time (min.)	thickness (μm)	σ_p(AM1) ($\Omega^{-1}cm^{-1}$)
K4030	0	420	24	26	0.4	2.1×10^{-5}
K4031	0.05	420	24	33	0.4	1.1×10^{-5}
K4032	0.2	420	24	36	0.4	5.1×10^{-6}
K4013	0.5	420	30	60	0.4	7.9×10^{-6}

*added in the form 1%NO in He

3.4 HYDROGEN CONCENTRATION AND BONDING

The nuclear reaction technique employing the resonance $^{1}H(^{19}F, \alpha\gamma)^{16}O$ has been used to accurately determine the hydrogen content of a-Si:H films produced by the static CVD of disilane. The hydrogen depth profile of an intrinsic film deposited at a substrate temperature of 420°C is shown in Fig. 5. The apparent modulation of the hydrogen concentration is real and is explained below.

The a-Si:H exhibits infrared absorption bands at 2070, 1995, 810, and 610 cm^{-1}. We have assigned the peak at 2070 cm^{-1} to the SiH_2 stretch mode, the peak at 1995 cm^{-1} to the SiH stretch mode, and the peak at 610 cm^{-1} to silicon-hydrogen bending and wagging modes. As the substrate deposition temperature increases the 2070 cm^{-1} peak decreases relative to the 1995 cm^{-1} peak and disappears at 430°C.

3.4 HYDROGEN AND OXYGEN DEPTH PROFILE

In this contract static CVD methods have been investigated. In our new contract flow CVD methods will be investigated. In CVD both homogenous gas-phase and heterogeneous gas-surface reactions can be important. At the beginning of the CVD process the reactants start breaking up, the process is fairly simple, and the growth rate is low. However, as the CVD process continues the growth rate increases and complicated new species are generated which can be important in determining the properties of the deposited material. Still later in the CVD process the growth rate decreases and the chemistry becomes less complicated in the sense that most of the reactants have been consumed and stable products and by-products have been formed. In the static method all these vastly changing reaction conditions contribute to the film deposition.

A SIMS depth profile of a 0.5 micron thick a-Si:H film deposited by CVD in a static system revealed the hydrogen concentration to be modulated with 4 peaks (see Fig. 6). The film was grown using four disilane pressurizations. The system is evacuated before each pressurization. These interesting results imply that in the region of high growth rate or rich gas-phase chemistry that a higher hydrogen concentration is found in the film.

The oxygen profile is also modulated but with a subtly different shape and the peak concentration occurs in the interface regions (substrate/film, film/film repressurization layers, and film/surface).

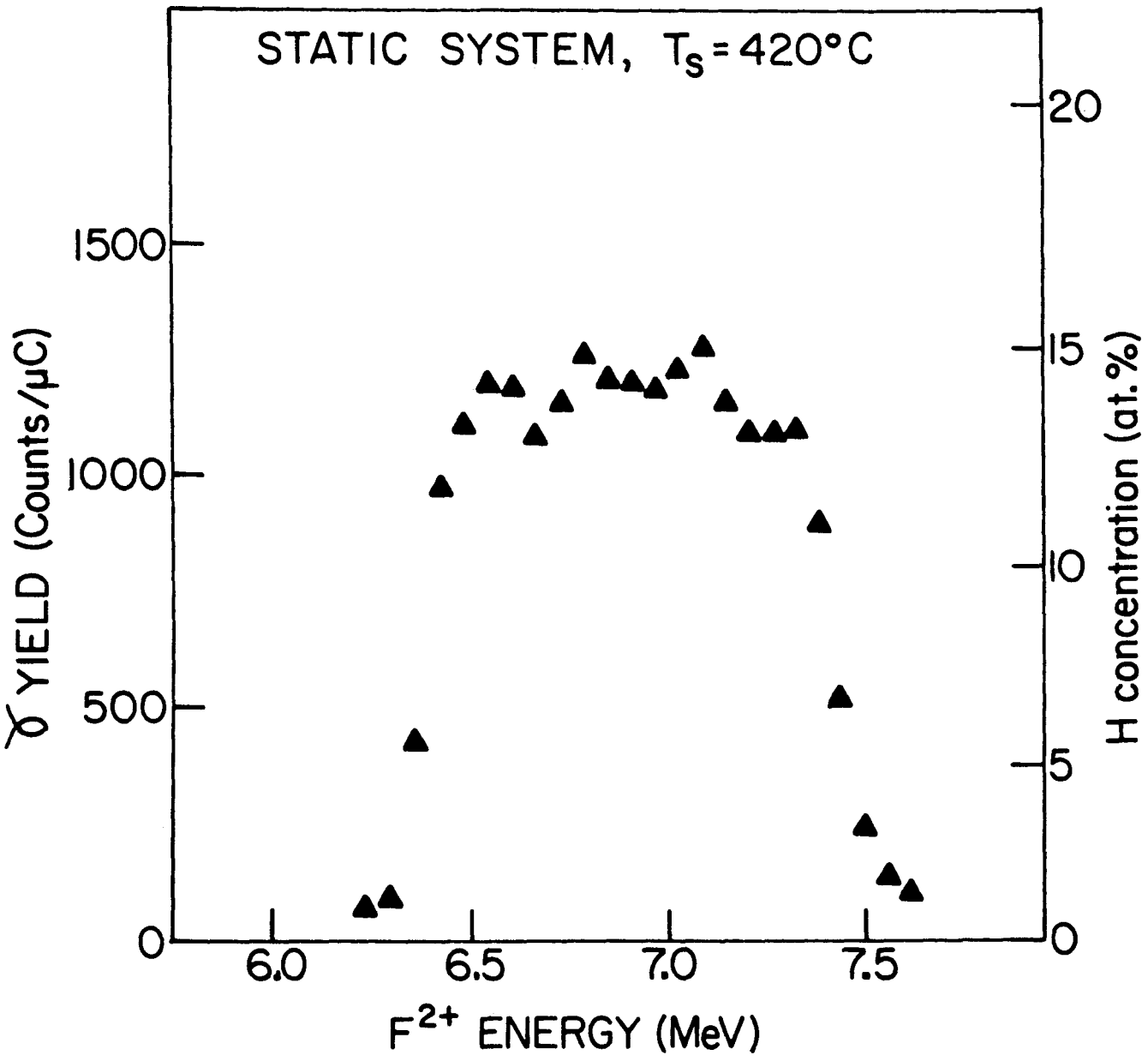

FIG. 5. Hydrogen depth profile from nuclear reaction technique of an a-Si:H film prepared by the CVD of diailane.

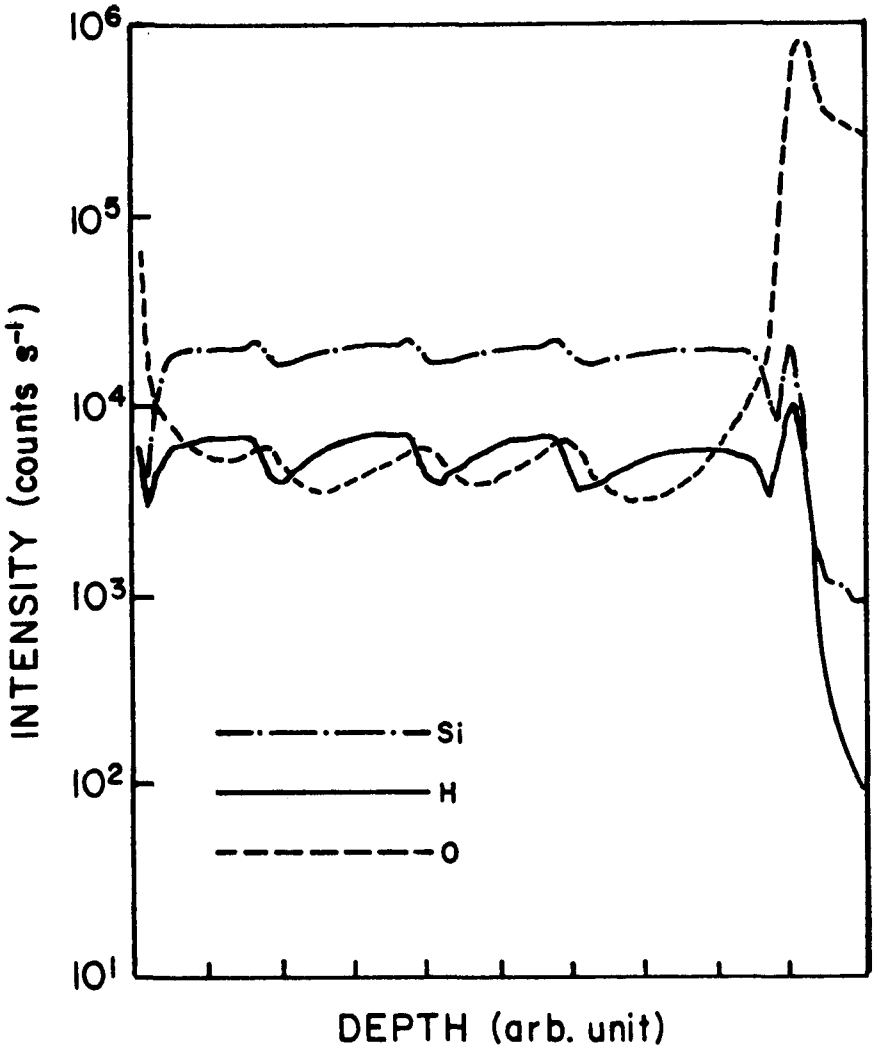

FIG. 6. SIMS depth profile of an a-Si:H film deposited in a static system by the CVD of disilane.

SECTION 4
MATERIAL AND DEVICE DEVELOPMENT

4.1 RESIDUAL DOPANT EFFECT

The pronounced effects on the electronic properties of a-Si:H due to residual dopants in the deposition chamber are well known in the case of glow discharge deposition. However, in the case of CVD it is conceivable that such effects might be absent due to the absence of any plasma in contact with the walls of the system. To test this hypothesis, three separate runs were made on gap cell substrates--a standard i layer, followed by a heavily doped n layer (using phosphine), followed again by a standard i layer. All layers were 0.4 microns in thickness and were deposited using 4 cycles of pressurization of reaction chamber with gas, deposition of film, and evacuation of gas. The deposition chamber was pumped for 1.5 hours after the doped layer, but otherwise not cleaned in any way. The results are shown in Table II. A definite increase in the dark conductivity and photoconductivity of the second i layer is observed. We conclude that residual dopant effects also exist in the CVD process. The same experiment should be performed using diborane.

Table II. Deposition parameters and conductivities of films in residual dopant experiment.

run #	gas	T_s (^oC)	P (Torr)	Dep time (min)	σ_d ($\Omega^{-1}cm^{-1}$)	σ_p(AM1) ($\Omega^{-1}cm^{-1}$)
B1009	Si_2H_6	420	20	40	$7.3x10^{-10}$	$6.2x10^{-6}$
B1010	Si_2H_6+ 20%PH_3	420	20-96	121	$5.3x10^{-2}$	$2.6x10^{-3}$
B1011	Si_2H_6	420	20	35	$3.7x10^{-8}$	$1.3x10^{-5}$

4.2 CONTAMINANTS IN DISILANE

The use of proprietary molecular sieves designed to remove or trap water, hydrochloric acid, oxysilanes, chlorosilanes, and hydrocarbons from disilane has been investigated. The i layer results are given in Table III. Unfortunately, the reason for the large difference in the dark conductivity and the photoconductivity for samples G1091 and G1092 is not known. The large photoconductivities for samples G1092-G1094 indicate

extrinsic doping (see below). Thus, as measured by the dark and photoconductivity, it appears that there is little difference between the purified and unpurified disilane.

Table III. I-layers deposited from trapped and untrapped disilane.

run #	disilane	pump	t (μm)	σ_d ($\Omega^{-1}cm^{-1}$)	σ_p(AM1) ($\Omega^{-1}cm^{-1}$)
G1091	untrapped	mechanical	0.24	$3.6x10^{-9}$	$6.5x10^{-7}$
G1092	untrapped	diffusion	0.24	$4.2x10^{-7}$	$1.4x10^{-5}$
G1093	trapped	mechanical	0.30	$1.8x10^{-8}$	$1.8x10^{-5}$
G1094	trapped	diffusion	0.35	$4.2x10^{-8}$	$1.3x10^{-5}$

However, Table IV illustrates the surprising results for purified (trapped) versus unpurified (untrapped) disilane in photovoltaic devices. In this case, the unpurified disilane is clearly superior. It is conceivable that the molecular sieves are contaminated and introduce an impurity which substantially degrades the photovoltaic properties of the i layer . However, as noted below, the photoconductivity of the CVD i layer is generally inferior to the photoconductivity of glow discharge material and there is some indication that deliberate ppm doping of the CVD i layer improves the efficiency of CVD pin devices by reducing the series resistance.

Table IV. Photovoltaic parameters for cells produced from trapped and untrapped disilane.

run #	disilane	pump	V_{oc} (V)	J_{sc} ($mAcm^{-2}$)	FF	Eff (%)
G1096	trapped	mech.	.453	2.44	0.341	0.376
G1097	untrapped	mech.	.614	5.25	0.311	1.00

4.3 SYSTEM CONTAMINANTS

Experiments were performed to determine whether the base pressure of the deposition system has any influence on solar cell efficiency. For this purpose a static CVD system was upgraded by the addition of an ionization gauge and controller. Six runs were made using unpurified disilane to provide nominally identical pin cells with the structure Ag/pin/ITO/glass. In each case, the substrate temperature was 408 °C, and the dopant concentrations were 30% phosphine and 3% diborane. Three runs were made using a mechanical pump to evacuate the chamber prior to deposition, followed by three runs in which the chamber was pumped by a liquid-nitrogen trapped diffusion pump to 5×10^{-5} torr or lower. The results are given in Table V. Diffusion pumping of the system improved the average cell efficiency from 0.93% to 1.17%. The J-V characteristics and spectral response of cell M506 are shown in Figs. 7 and 8 respectively.

Table V. Photovoltaic parameters of pin cells produced in a system evacuated either by a mechanical pump or by a diffusion pump.

run #	pump	V_{oc} (V)	J_{sc} (mAcm^{-2})	FF	Eff (%)	R_s (Ωcm^2)
M501	mech.	.628	5.10	0.279	0.895	115
M502	mech.	.626	5.09	0.299	0.953	95
M503	mech.	.583	5.02	0.321	0.937	77
M504	diff.	.578	5.37	0.336	1.04	63
M505	diff.	.575	6.03	0.322	1.11	62
M506	diff.	.624	5.94	0.368	1.36	52

4.4 MODIFICATION OF I LAYER PROPERTIES

4.4.1 Disilane-Water Vapor Mixtures

Schottky barrier solar cells were fabricated in the configuration Au/i-n a-Si:H/ITO/glass with nominally identical n layers, but having one of the i layers deposited in the usual way from disilane and the other deposited from a mixture of 95 % disilane and 5% water vapor. The respective spectral response of these cells is shown in Figs. 9 and 10 (illumination is from the Au side). A useful technique for examining transport in the i layer is to plot the ratio of the quantum efficiencies for two different voltage biases as a function of wavelength.[2] For the standard cell we deduce from the ratio shown in Fig. 9 that electron transport to the back n layer limits carrier collection. For the disilane-water vapor mixture exactly the opposite result is obtained--here hole transport to the front Au contact is limiting. Thus like oxygen water dopes n type.

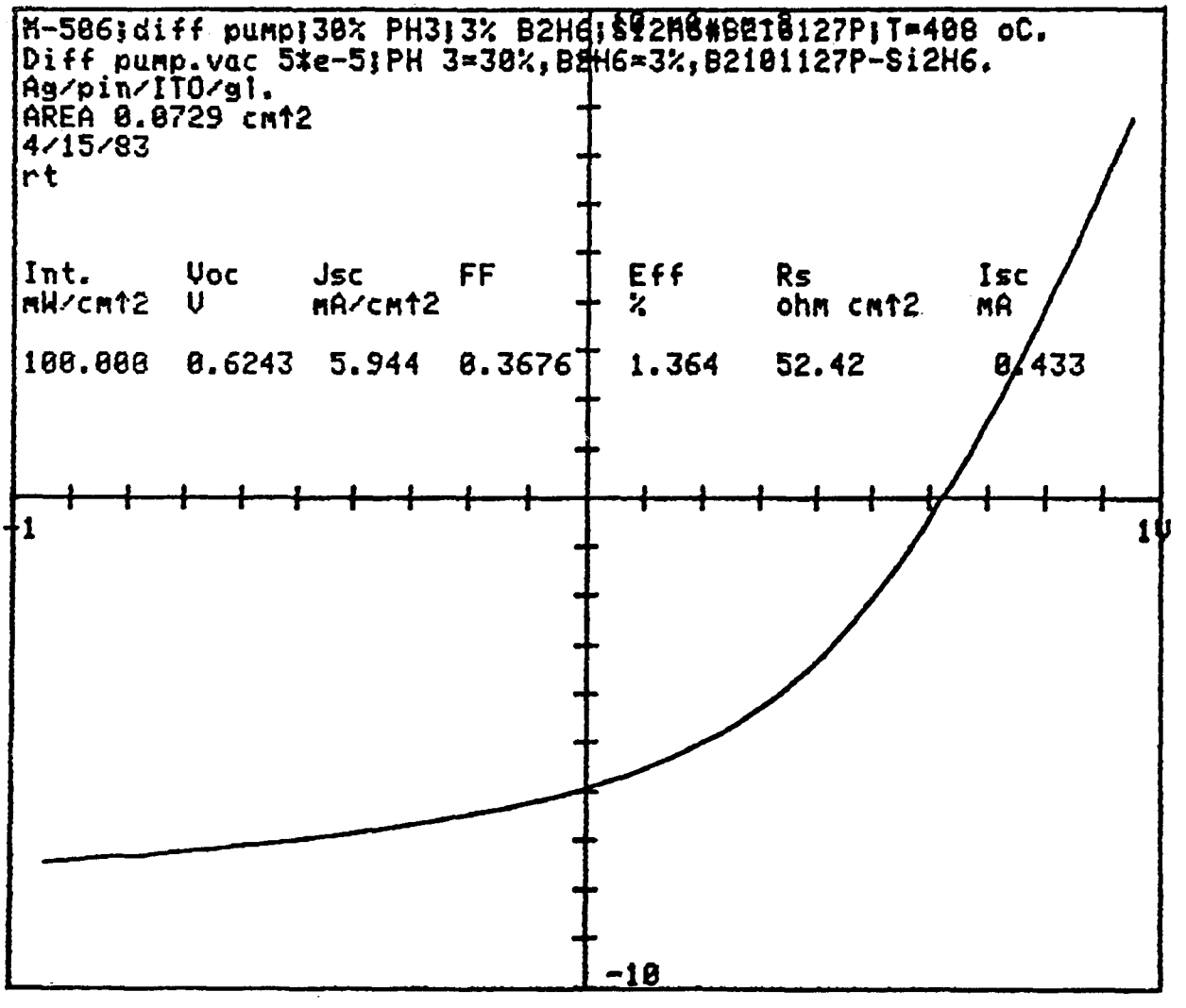

FIG. 7. J-V characteristics under AM1 illumination for pin cell M506.

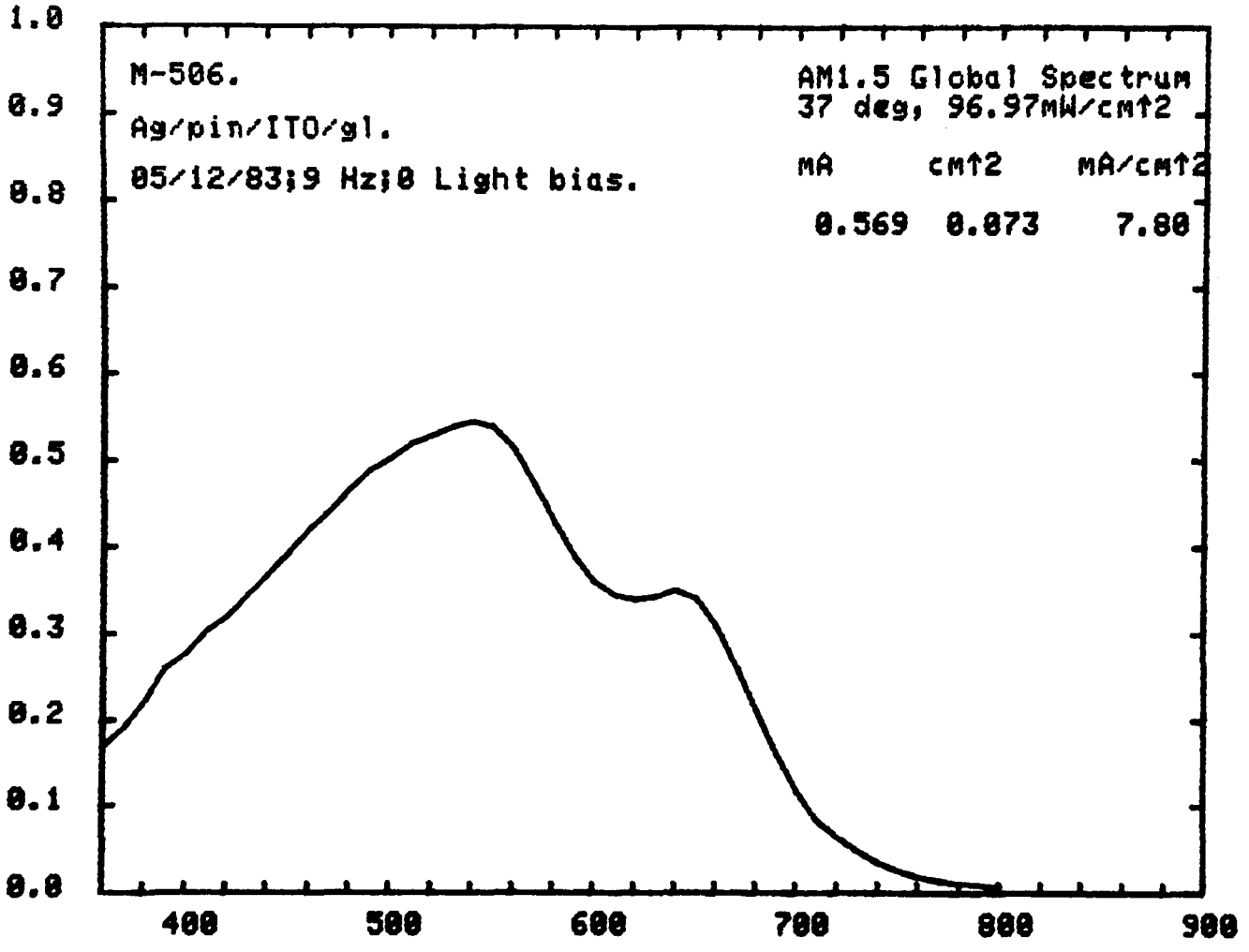

FIG. 8. Spectral response of pin cell M505.

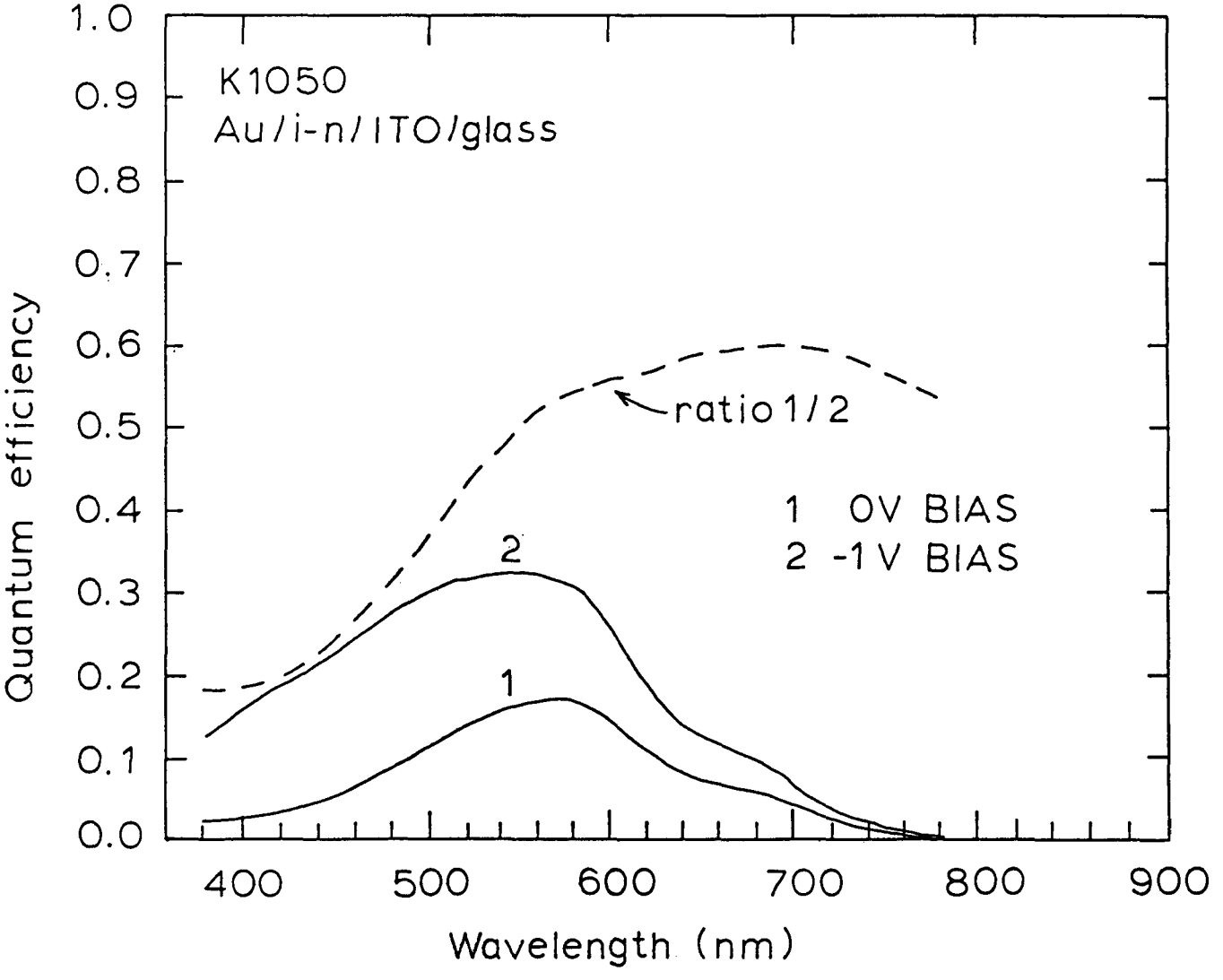

FIG. 9. External quantum efficiency versus wavelength for a Au Schottky CVD a-Si:H solar cell deposited from disilane.

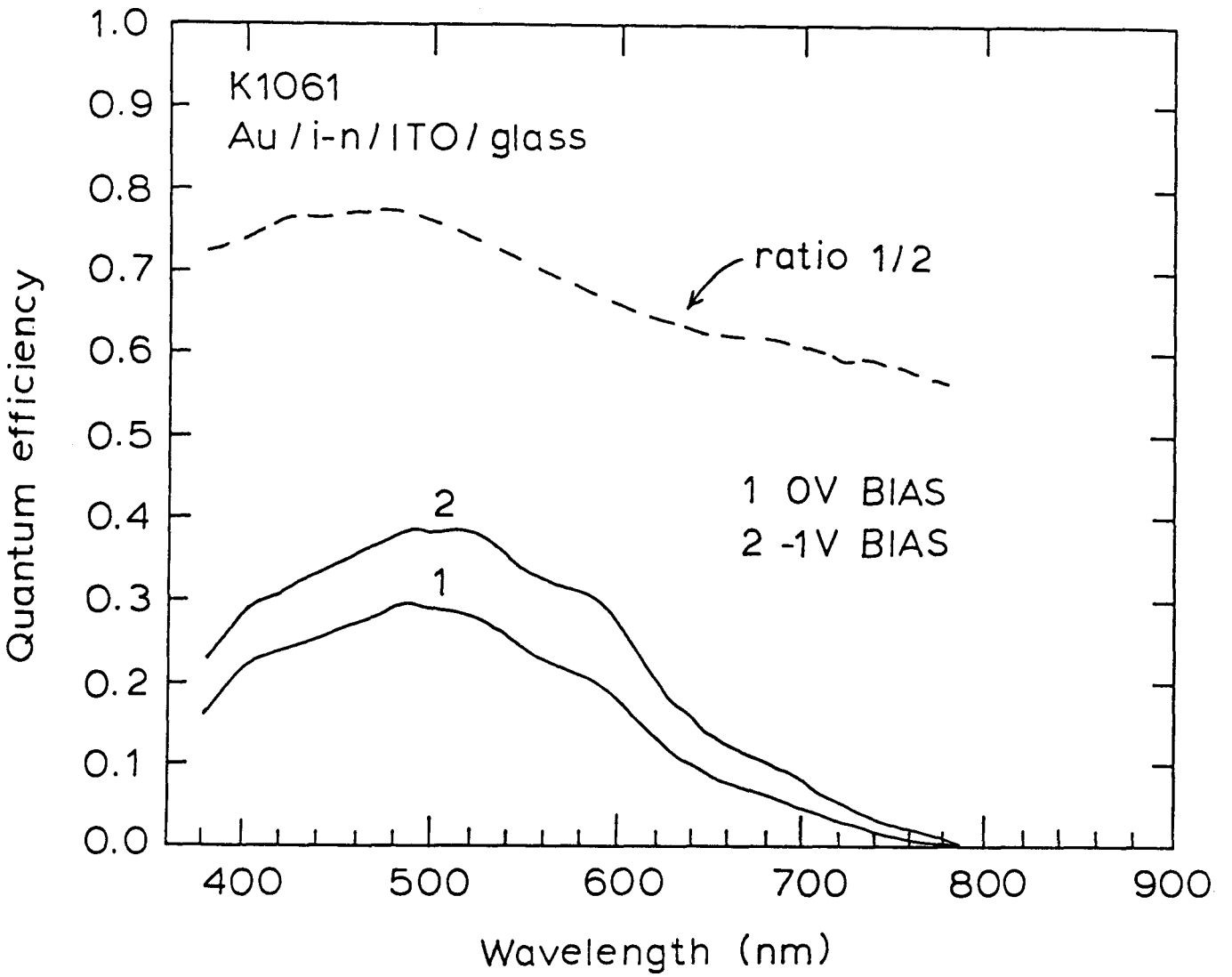

FIG. 10. External quantum efficiency versus wavelength for a Au Schottky a-Si:H cell deposited from 95% disilane and 5% water.

4.4.2 Ppm Phosphine Doping

In an early study of ppm phosphine doping of the i layer, we discovered that the photoconductivity of the i layer increases (see below) and that the fill factor of Schottky devices improves. Presumably this result is a direct consequence of the reduction in series resistance due to the increase in photoconductivity.

More recently, experiments were again performed to test the effect of ppm doping of the i layer by phosphine. 50 ppm phosphine was added to the disilane and two substrate temperatures (408 and 428 °C) were compared. Both Au and Au/Pd Schottky barrier devices were fabricated on each run. The efficiency of the Au devices was approximately double that of the Au/Pd devices. The results for the Au devices are shown in Table VI. The best devices were obtained at 428 °C using pure disilane. These results indicate that 50 ppm phosphine reduces both the short-circuit current and the open-circuit voltage, and that the fill factor significantly increases. It may be that a lower phosphine concentration would be sufficient to increase the fill factor without adversely affecting the short-circuit current and open-circuit voltage. The effect of ppm diborane and a graded combination of ppm phosphine and diborane doping remains to be investigated.

TABLE VI. Photovoltaic parameters of Schottky barrier solar cells having i-layers grown under different conditions.

T_s (°C)	Gas*	V_{oc} (V)	J_{sc} ($mAcm^{-2}$)	FF	η (%)
408	A	0.423	2.54	0.374	0.401
428	A	0.441	2.87	0.457	0.579
408	B	0.405	1.89	0.435	0.333
428	B	0.383	2.27	0.468	0.407

*A: pure Si_2H_6

B: Si_2H_6 + 50 ppm PH_3

4.5 PHOTOCONDUCTIVITY

We have completed a thorough set of photoconductivity measurements on our undoped material. We find a systematic change in photoconductivity with dark Fermi level position. As the Fermi level moves towards the conduction band, the photoconductivity increases. This behavior is shown in Fig. 11 as a universal curve for the photoconductivity versus the Fermi level. This result is similar to the result for glow-discharge a-Si:H films (see, for example, data from the Brookhaven group) and arises from the fact that a movement of the Fermi level upwards reduces the density of electron recombination centers, hence increasing the mobility-lifetime product for electrons.

The mobility-lifetime product ($u_n \tau_n$) for electrons was calculated from the photoconductivity (σ_p) measured at 600 nm using the equation

$$\sigma_p = (1-R)(1-e^{-\alpha x})(u_n\tau_n + u_p\tau_p)eF/x$$

and assuming $u_n \tau_n >> u_p \tau_p$. Here R is the reflectivity of the a-Si:H, α is the absorption coefficient, x is the film thickness, e is the electron charge, and F is incident photon flux. At an activation energy of 0.58 eV (calculated from the slope of an Arrhenius plot) mobility-lifetime products up to 2.2×10^{-7} cm^2V^{-1} have been obtained. Other examples of the mobility-lifetime product are 7.8×10^{-8} and 4.1×10^{-9} cm^2V^{-1} for activation energies of 0.63 and 0.73 eV respectively. These values are about one to two orders of magnitude smaller than those generally obtained with glow-discharge a-Si:H.

The temperature dependence of the photoconductivity exhibits a high temperature peak and falls off monotonically with decreasing temperature (see Fig.12, solid curve). From the high temperature (temperature greater than the temperature of the peak photoconductivity) activation energy of the photoconductivity we have concluded that the principal recombination centers lie approximately 0.96 eV below the conduction band edge. These centers are almost certainly silicon dangling bonds. A second low temperature peak in the photoconductivity has never been observed in the as deposited CVD films, while one is often observed in glow-discharge films,[3] reflecting a difference in gap state densities between the two materials. However, exposure of a CVD a-Si:H film to a glow discharge in hydrogen and argon did result in a second peak in the photoconductivity at about 0 °C.[4]

The excitation spectrum (spectral response of the photoconductivity) of the CVD films has also been measured. It clearly reveals a shift of the absorption edge to longer wavelengths relative to glow-discharge films. The absorption edge also shifts as a function of temperature, as shown in Fig. 13.

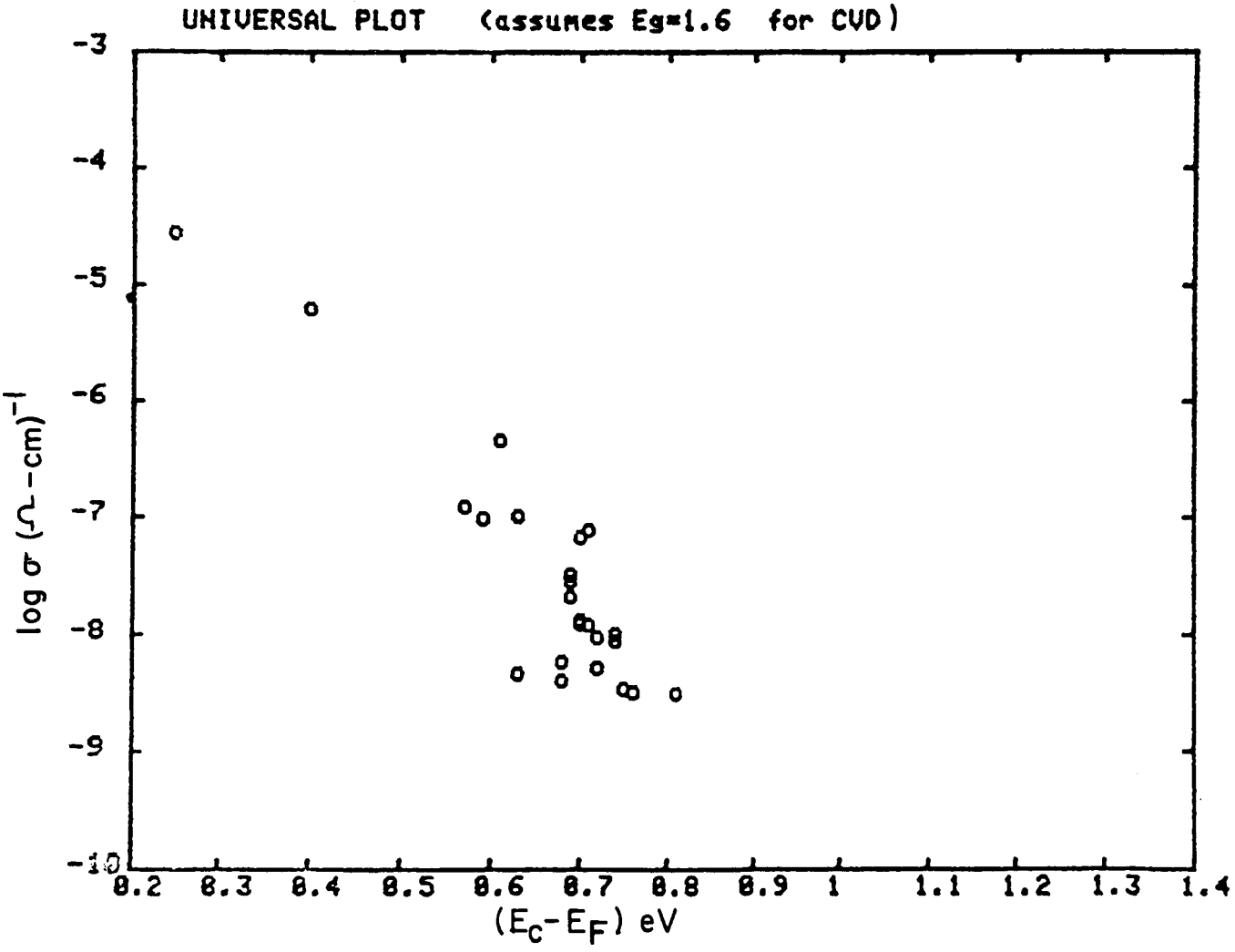

FIG. 11. Dark conductivity versus the position of the Fermi level.

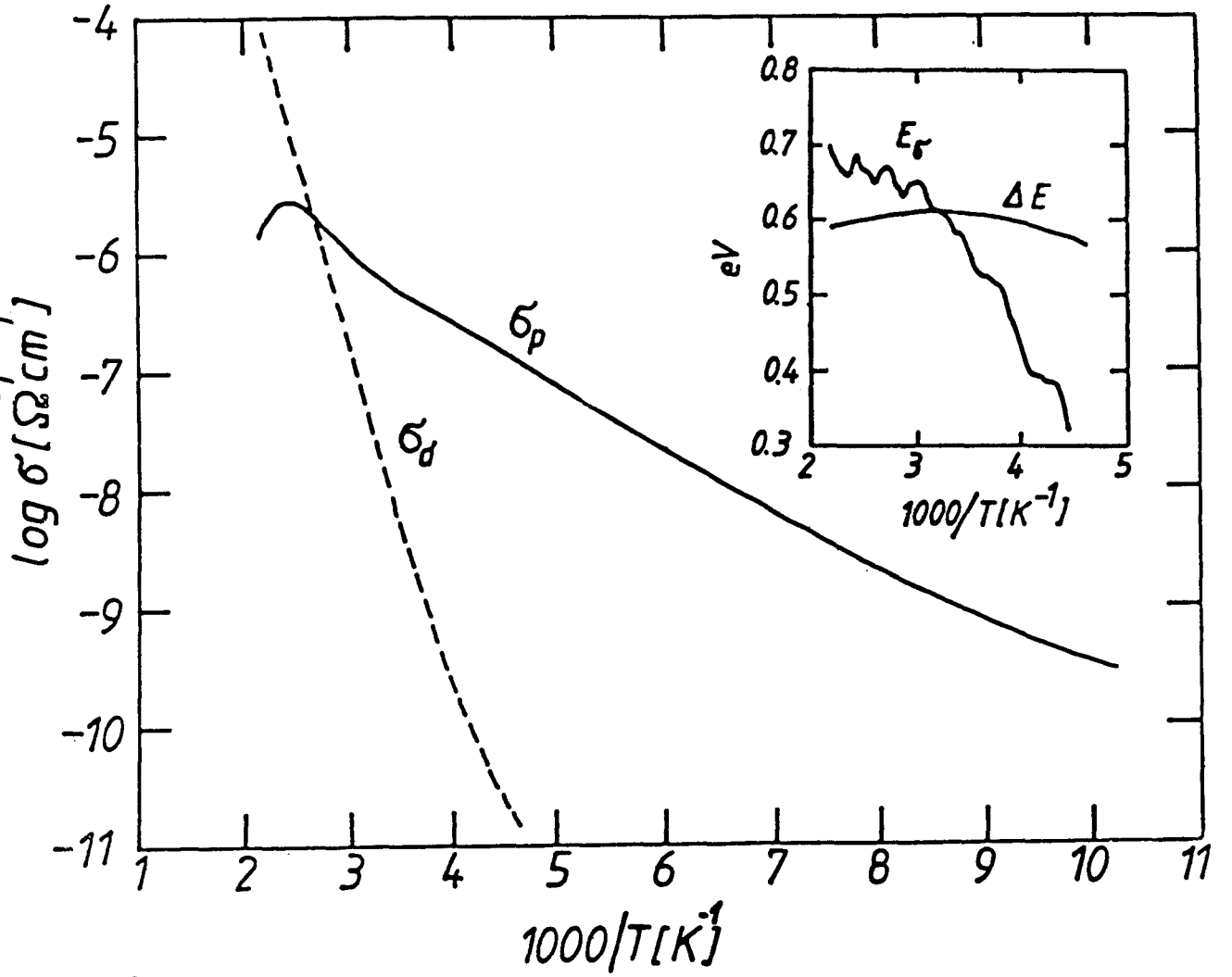

FIG. 12. Temperature dependence of the dark conductivity and photoconductivity of an intrinsic CVD a-Si:H film.

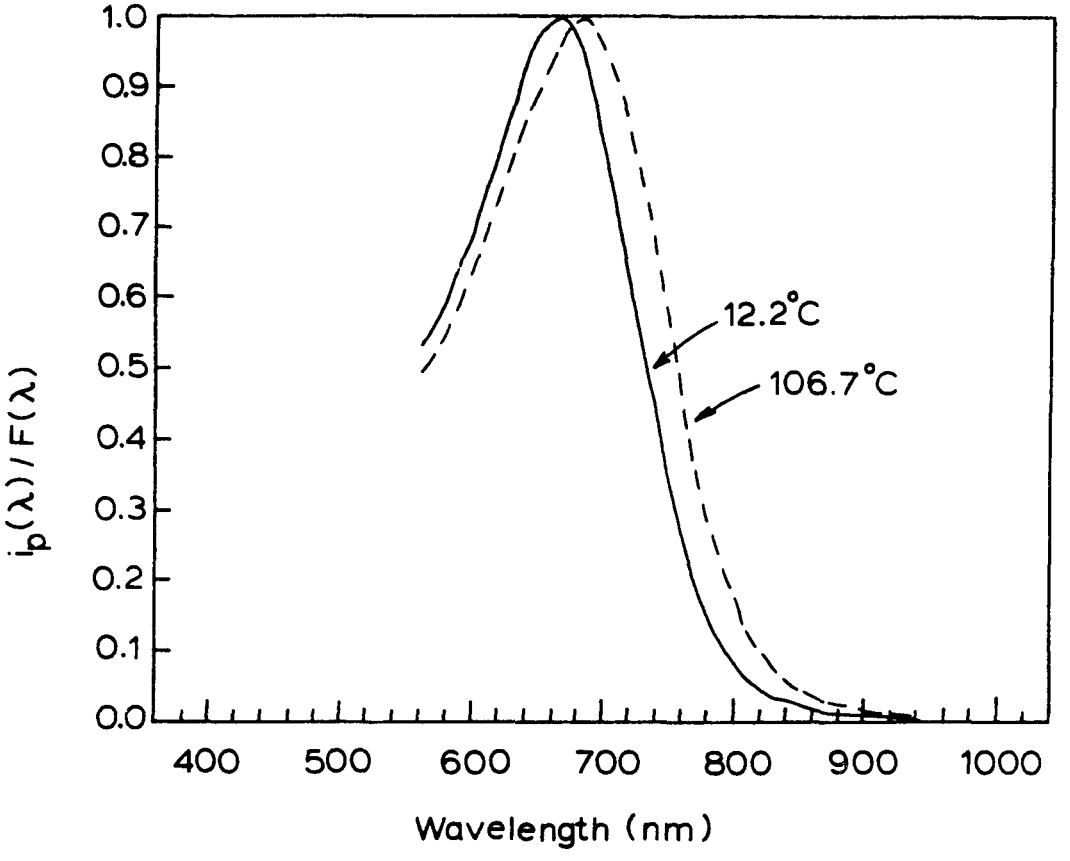

FIG. 13. Excitation spectrum of CVD a-Si:H showing shift of the absorption edge with temperature.

4.6 SUB-BANDGAP ABSORPTION

This weak absorption has been determined as a function of energy by measurement of the photoconductivity of CVD a-Si:H in the gap cell configuration using sub-bandgap light. For these measurements a chopped monochromatic source is superimposed on a red bias light of considerably higher intensity. Under these conditions, and provided that the light is weakly absorbed, the monochromatic component of the photoconductivity is proportional to $u_n\tau_n F(E)\alpha(E)$, where $u_n\tau_n$ is now fixed by the bias light and $F(E)$ and $\alpha(E)$ are, respectively, the monochromatic light flux and absorption coefficient. Thus, for weakly absorbed light, a plot of the photocurrent per incident photon versus photon energy will be proportional to the absorption coefficient. This is shown in Fig. 14. An exponential absorption edge of the form $\alpha = \alpha_0 \exp(E/E_0)$ is evident. It is generally accepted that E_0 is a measure of the disorder (thermal plus structural) in the film.[5] Raising the temperature of the film increases the thermal disorder and so E_0 increases, as shown in Fig. 14. It was found that the extrapolated absorption edges intersected at a fixed point (E_1,α_1), implying

$$\alpha(E,T,y) = \alpha_1 \exp((E-E_1)/E_0(T,y))$$

where y is the structural disorder parameter. More extensive data are presented in Fig. 15, where the variation with temperature of both E_0 and the energy gap (E_g) are shown. The slopes of these lines are $\partial E_0/\partial T = 7.2\times10^{-5}$ eV/°C and $\partial E_g/\partial T = -5.2\times10^{-4}$ eV/°C. This implies $\Delta E_g/\Delta E_0 = -7.2$. An almost identical value of $\Delta E_g/\Delta E_0$ was obtained from measurements made at room temperature on films deposited at different substrate temperatures. This remarkable result strongly suggests that the energy gap is determined by E_0, and hence by the disorder in the film. The value of E_0 is about thirty percent larger in CVD films than in glow-discharge films, implying a wider valence band tail in the CVD material.

4.7 STACKED CELLS

For CVD devices stacked, multiple-junction, series connected cells may be preferred, in spite of the more complicated processing and current losses due to absorption in the several n and p layers, since:

1. Stacked, multiple-junction cells increase voltage and reduce current. To a first approximation, the voltage to current ratio increases as n^2, where n is the number of cells in a stack. Hence, series resistance loss which is IR/V reduces as $1/n^2$. Thus, provided that the contact resistance between the n and p layers is low, stacked cells furnish a good method for increasing the fill factor in spite of the lower photoconductivity of the CVD material.

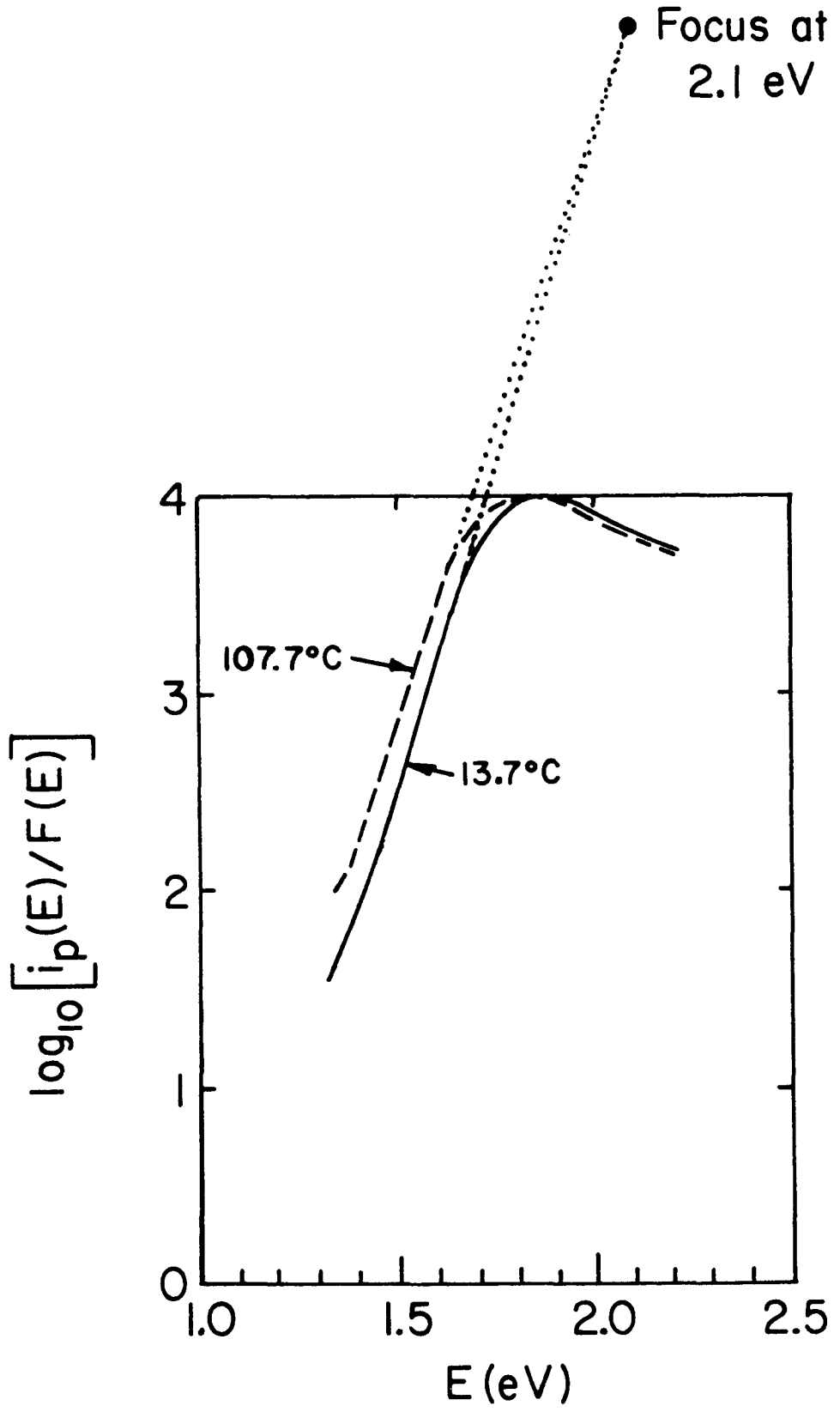

FIG. 14. Photocurrent per incident photon versus photon energy for CVD a-Si:H at two temperatures. For E < 1.6 eV, this curve essentially represents the optical absorption coefficient of the material.

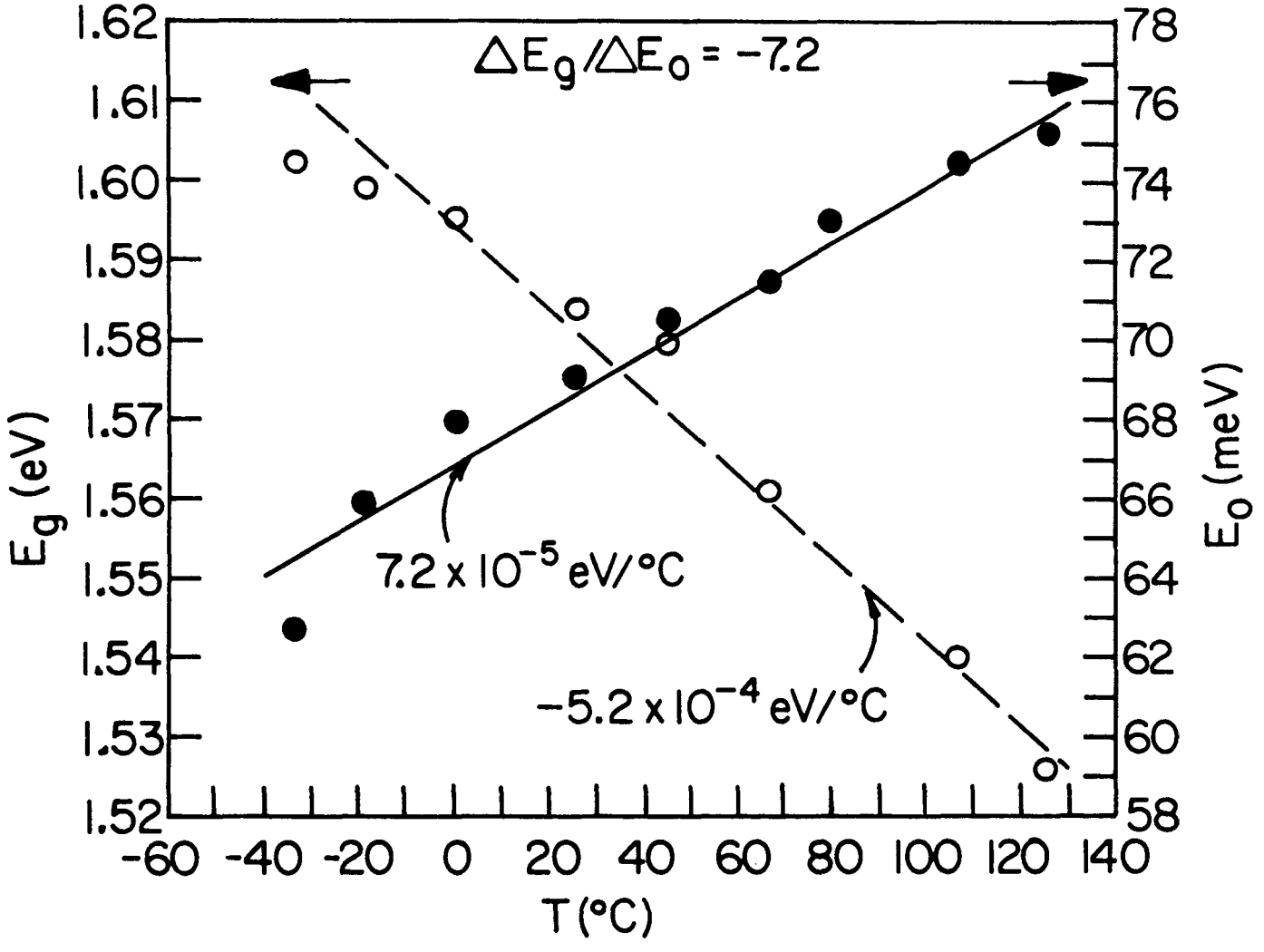

FIG. 15. Variation with temperature of the energy gap, E_g (open circles) and the inverse slope of the absorption edge, E_o (closed circles).

2. By using multiple junctions in series, the thickness of i layers can be reduced for approximately the same total efficiency. Thus, stability improves, since the electric field is now higher in the thinner layers.

Triply stacked CVD pin solar cells have been produced with efficiencies greater than three percent.

4.8 DOPED LAYERS

4.8.1 Boron Doped Layers

A new p a-Si:H material was developed by using the catalysis of monosilane by diborane. Monosilane and diborane were mixed in a manifold and were continually passed into a quartz hot-wall reactor maintained at 440 C (outside temperature). The typical flow rates were such that the residence times in the hot zone were only a few seconds. Perfectly specular, very inert films were obtained. The diborane to monosilane ratio was varied between 0.1 and 10 percent. The resultant room temperature conductivity data are shown in Fig. 16. The highest conductivities are in the range of $7x10^{-4}$ $(ohm-cm)^{-1}$, with an activation energy of about 0.3 eV.

Using a ratio of diborane to disilane of one percent, a p layer is obtained with a dark room temperature conductivity of $1.1x10^{-3}$ $(ohm-cm)^{-1}$ and an activation energy of about 0.25 eV.

4.8.2 Wide Band Gap Boron Doped Material

Boron doped a-Si:H alloys can be deposited by heating a mixture of diborane and silanes. However, the decomposition of diborane catalyzes the decomposition of the silanes resulting in very high and often less controllable deposition rates. Employment of substituted silanes, e.g., methylsilane, has been found to offer the following advantages:

1. Wide gap films can be obtained.

2. Thin photoconductive films can be obtained.

3. The deposition rate is slow and controllable.

As an example, 25 torr methylsilane and 1.5 torr diborane at 500° C yielded a 0.16 micron film with a band gap of 2.04 eV and photoconductivity (AM1) of $5.6x10^{-8}$ $(ohm-cm)^{-1}$. The film exhibited infrared absorption peaks at 2060 cm^{-1} (Si-H) and at 1260 and 810 cm^{-1} ($Si-CH_3$).

4.8.3 Phosphorous Doped Layers

A ratio of 11% for the phosphine to disilane concentration resulted in a film with a dark conductivity of $5.6x10^{-3}$ $(ohm-cm)^{-1}$ and an activation energy of about 0.2 eV.

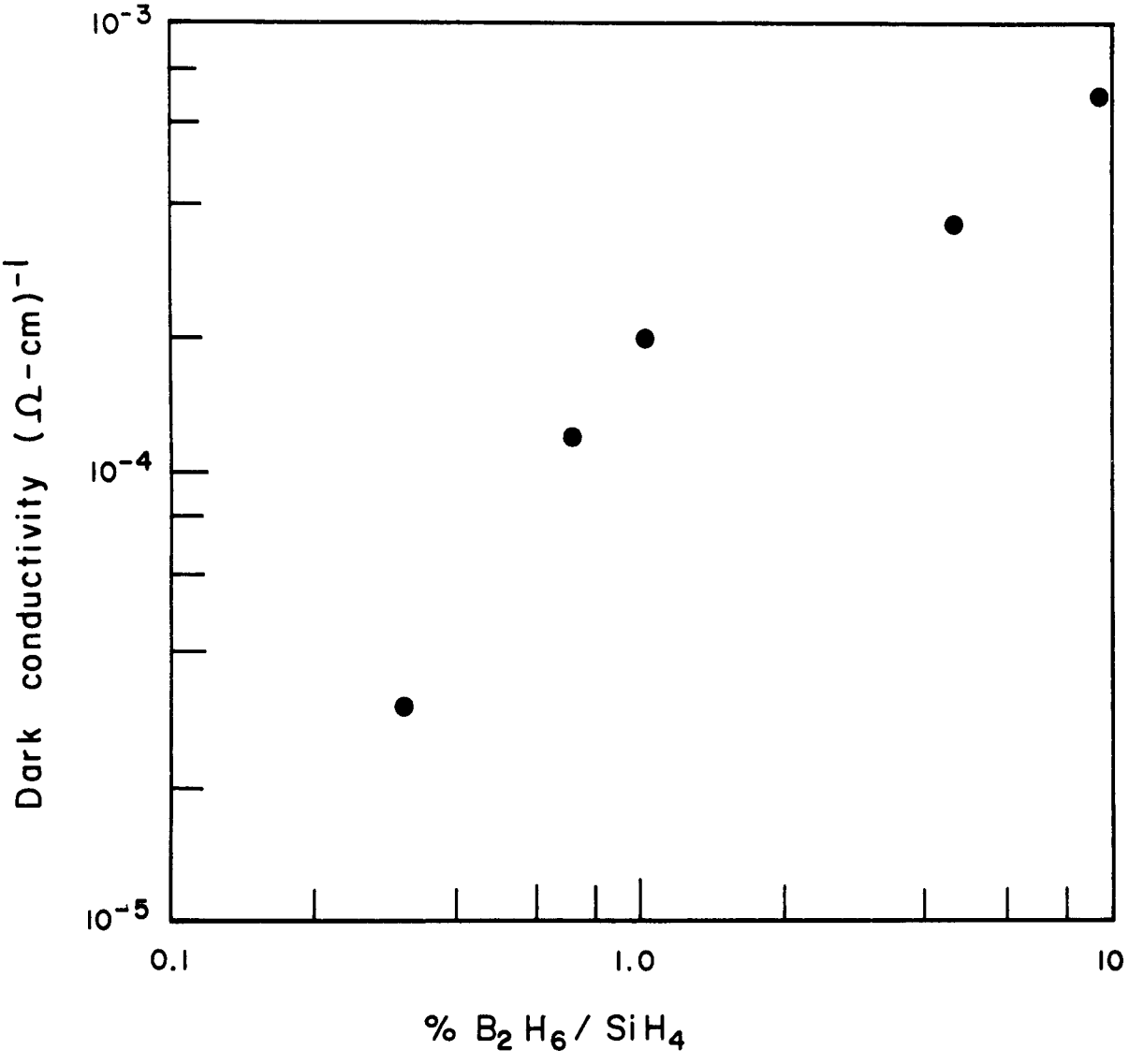

FIG. 16. Dark conductivity of p layers versus the ratio of diborane to monosilane.

SECTION 5
NEW DEPOSITION METHOD--PHOTO CVD

The higher deposition temperatures needed in thermal CVD, which may limit the film quality directly or indirectly through contamination by diffusion across the film/substrate interface, have prompted us to consider alternative deposition schemes for depositing a-Si:H. We have successfully grown highly photoconductive a-Si:H films by mercury sensitized deposition from disilane using UV light resonantly absorbed from mercury lamps.

$$Hg_6(^1S_0) + h\nu(253.7nm) \longrightarrow Hg_6(^3P_1)$$

The excited mercury atom exists in a comparatively long-lived triplet state, and can therefore undergo many collisions. It can abstract hydrogen from silanes, forming the unstable intermediate HgH which decomposes into mercury and atomic hydrogen. The atomic hydrogen can also abstract a hydrogen atom from silanes. Thus each excited mercury atom can lead to two silyl type radicals. As an example of a deposited film, a 1000 angstrom a-Si:H film deposited by this technique at a substrate temperature of 270 °C exhibited a band gap of 1.96 eV (see Fig. 17). However, because of the thinness of the layer the band gap measurement is about 0.1 to 0.2 eV larger than it would be for a film with the same properties but much thicker, say about 0.6 microns. The dark conductivity is 3.5×10^{-7} $(ohm\text{-}cm)^{-1}$, and the AM1 photoconductivity is 3.5×10^{-4} $(ohm\text{-}cm)^{-1}$.

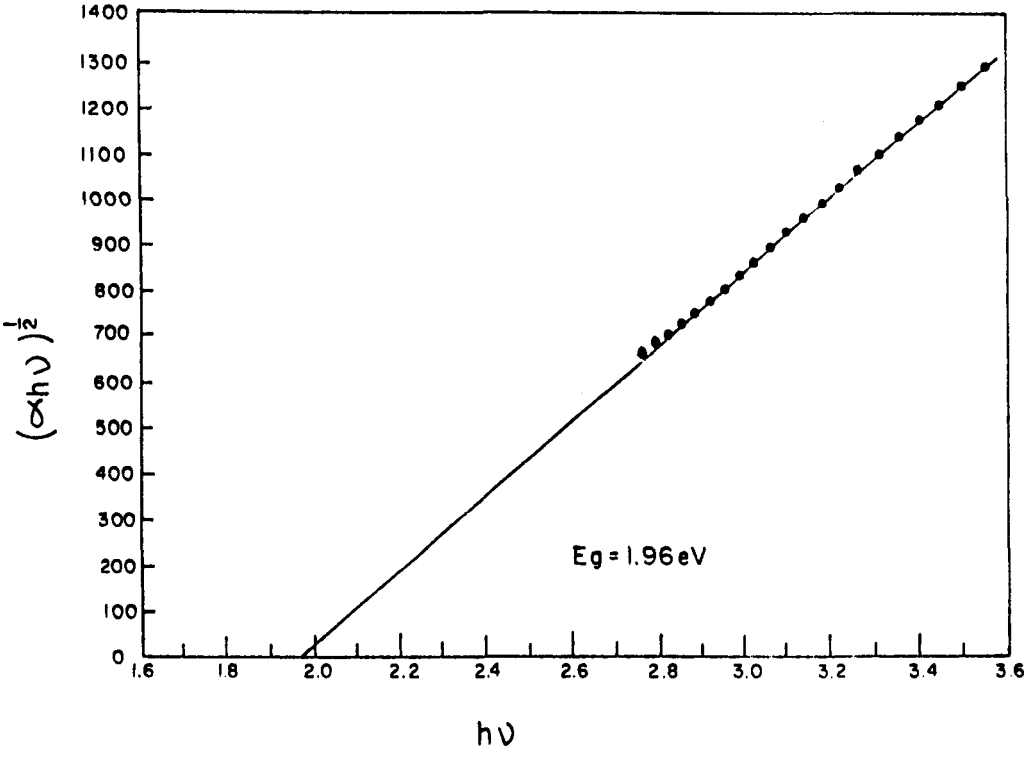

FIG. 17. Square root of the product of the absorption coefficient and the photon energy versus the photon energy for sample G-561, an a-Si:H film prepared by mercury-sensitized photoCVD of disilane.

SECTION 6
CONCLUSION

In this work the properties of a-Si:H produced mainly by the static CVD of disilane were examined in detail. In general the photoconductivity of the intrinsic layers was about an order of magnitude lower than acceptable for device application. The low photoconductivity introduces a series resistance which degrades the fill factor. Ppm doping of phosphine showed promise of improving the photoconductivity without necessarily compromising the short-circuit current. However, further research of ppm phosphine doping as well as exploring ppm diborane doping of the i layer needs to be done. The results of such doping may be different from what is obtained for material produced by other techniques, notably glow discharge, and may lead to significantly improved solar cell material.

It was found that the ratio of the change in inverse slope of the sub-bandgap absorption edge to the change in band gap was a universal constant independent of the method employed to effect these changes, strongly indicating that the energy band gap is determined by the disorder of the material. The inverse slope of the above edge is roughly 68 meV which is unacceptably high for good photovoltaic devices. In diagnostic solar cell devices, the short-circuit current was also unacceptably low, indicating a high gap state defect density in agreement with the sub-bandgap measurements.

A necessary but insufficient criterion for producing low gap state defect densities is a hydrogen concentration empirically found to be above about 5-10 atomic percent. At one time, because of the high CVD deposition temperatures, one expected the CVD material to suffer from insufficient hydrogen. This is not the case, since the atomic percent hydrogen is about 14 percent. However, it was discovered that the static CVD method with several repressurizations introduces a modulation of both the hydrogen concentration and oxygen concentration in the a-Si:H films. It is expected that this concentration modulation impairs the transport properties of the films. Future CVD of disilane will focus on flow methods which should eliminate this problem.

Doped n and p type layers with high room temperature dark conductivities (10^{-2}-10^{-4} $ohm^{-1}cm^{-1}$) and low activation energies were obtained (0.2-0.3 eV). In addition, a wide band gap p layer was obtained using methylsilanes which may have interesting device application.

Work on the mercury sensitized photo CVD of disilane was commenced. This technique produces a-Si:H films and we believe it to be a very promising new technique since low deposition temperatures are possible and since atomic hydrogen is produced. Future work will focus both on the film properties and altering the deposition system to permit the deposition of thicker films.

SECTION 7
REFERENCES

1. B. Scott, R.M. Plecenik, and E.E. Simonyi, Appl. Phys. Lett 39, 73 (1981).

2. A.E. Delahoy and R.W. Griffith, Conference Record of the 15th IEEE Photovoltaic Specialists Conference, May 1981, Kissimmee, Florida, 704 (IEEE, New York 1981).

3. P.E. Vanier, A.E. Delahoy, and R. W. Griffith, J. Appl. Phys., 52, 5235 (1981).

4. A.E. Delahoy, "Properties of Hydrogenated Amorphous Silicon Prepared by Chemical Vapor Deposition from Higher Silanes", Photovoltaics for Solar Energy Application II, D. Adler, Editor, Proc. SPIE 407, 47 (1983).

5. G.D. Cody, T. Tiedje, B. Abeles, B. Brooks, and Y. Goldstein, Phys. Rev. Lett. 47, 1480 (1981).

SECTION 8
PERSONNEL

A. E. Delahoy	Principal Investigator/Program Manager March 1, 1983 - August 31, 1983
V. L. Dalal	Principal Investigator/Program Manager August 1, 1982 - February 28, 1983
M. Akhtar	Scientist
A. Vaseashta	Research Associate
T. Rotberg	Technician
K. Mahmood	Technician

ACKNOWLEDGEMENTS

We appreciate and thank Mr. A. Lichter for the in-house preparation and purification of the higher silanes, Dr. F. B. Ellis, Jr., for his generous assistance in the preparation of this report, Dr. P. S. Peercy at Sandia National Laboratory for the nuclear reaction analysis, and SERI for the SIMS analysis.